# EXPERIMENTAL INVESTIGATION OF ULTRA WIDEBAND DIVERSITY TECHNIQUES FOR ON-BODY RADIO COMMUNICATIONS

## Q. H. Abbasi[1, 2] *, M. M. Khan[2], S. Liaqat[1], M. Kamran[1], A. Alomainy[2], and Y. Hao[2]

[1]University of Engineering and Technology, Lahore, Pakistan

[2]Queen Mary, University of London, UK

**Abstract**—This paper presents an experimental investigations and analyses of ultra-wideband antenna diversity techniques and their effect on the on-body radio propagation channels. Various diversity-combining techniques are applied to highlight; how the overall system performance may be enhanced. Diversity gain is calculated for five different on-body channels and the impact of variation in the spacing between diversity branch antennas is discussed, with an emphasis on mutual coupling, correlation and power imbalance. Results demonstrate the repeatability and reliability of the analysis with error variations as low as 0.8 dB. The study highlights the significance of diversity techniques for non-line-of-sight propagation scenarios in body-centric wireless communications.

## 1. INTRODUCTION

Ultra-wideband (UWB) is an innovative wireless technology capable of transmitting digital data over an extremely wide frequency band with very low power and very high data rates. The wide-bandwidth nature of the technology implies the transmission of short pulses; this, in turn, gives rise to a broad distribution in the time-of-arrival characteristics of these pulses, when considering multipath components in an indoor environment. Hence, this reduces interference, as it is easier to distinguish multipath components than in narrow-band systems operating in a similar environment.

Wireless body area networks (WBANs) mainly experience fading due to the following: relative movements of body parts; polarisation

mismatch; shadowing; and diffraction and scattering from the body parts and surrounding environments [1, 2]. Diversity is a powerful technique to combat fading and multipath effects [3]. Antenna diversity [3, 4] can be achieved either by using different radiation patterns, different polarisations, or both; or by varying the spacing between the antennas (spatial diversity) at the transmitter, or receiver, or both. Spatial diversity does not need any additional spectrum [3, 5] as compared to other diversity techniques like frequency or time etc.; in addition, UWB is inherently a frequency diversity technology. This makes the spatial arrangement of multiple antennas a promising technique to enhance the performance of body-centric wireless networks [6].

In the work presented here, spatial diversity is experimentally investigated for UWB on-body communication channels. The improvement due to diversity is often measured in terms of *diversity gain* (DG); this is basically an improvement in signal strength (or, equivalently, signal-to-noise ratio or bit-error rate) compared with that observed with a single antenna at a certain outage probability [2, 3, 5, 7, 8]. The outage probability is the probability that the system performance falls below a minimum performance threshold (typically defined in terms of signal-to-noise ratio) within a specified time period [9]. There has been an increasing interest in diversity and multiple-input, multiple-output (MIMO) techniques for enhanced mobile and wireless communications in recent years [5, 7, 8, 10–12]. An experimental investigation of diversity antennas has been presented in [10], with results showing that, for non-line-of-sight (NLOS) scenarios, diversity gains of up to 10 dB can be achieved, at an outage probability of 1%. There are some studies presented in the open literature where the benefits of diversity techniques for on-body communications in narrow-band systems have been investigated [2, 13–15]. Introductory studies for on-body diversity measurements at 2.45 GHz were presented in [13]. The diversity performances were evaluated in terms of DG, power imbalance and envelope correlation coefficients between the two receiving channels. A comprehensive study of diversity for an on-body channel at 2.45 GHz was presented in [2], using different antennas and diversity types. A significant gain was observed for NLOS channels and dynamic channels involving large body movements. The uplink and downlink diversities were also calculated and found to be similar. Cotton and Scanlon [14, 15] have presented first- and second-order statistics and some diversity results for off-body and on-body channels, at 2.45 GHz and 868 MHz, respectively. On-body diversity at 868 MHz has been thoroughly investigated in [15], with application to medical implants.

Other studies on UWB-MIMO and UWB diversity were presented in [16–23]. Antenna diversity results for the UWB indoor channel are presented in [19], with an emphasis on differences between virtual and real compact arrays, including mutual coupling effects. UWB-MIMO for on-body has been investigated in [17], using frequency-space polarization. The key findings in [17] were that, in WBANs, the MIMO channel capacity is mainly determined by the power imbalance for both spatial arrays and polar arrays. It was also found that the MIMO capacity decreases with the frequency. Roy et al. presented an innovative space-time spatial model for UWB multi-sensor, multi-antenna BANs in [23]. However, to the authors' knowledge, UWB spatial diversity for on-body communications has not yet been investigated systematically and thoroughly. The initial studies on UWB diversity for BANs is being presented by authors in [24, 25].

This paper presents detailed studies for UWB spatial diversity both in an anechoic chamber and in an indoor environment, using different antenna spacings, locations (of the human subjects in an indoor environment) and positions of the antennas on the human subjects. The rest of the paper is organized as follows. Section 2 describes the measurement campaign adopted in this study. Section 3 presents a diversity technique analysis for UWB on-body radio channels. In Section 4, the effect of different scenarios and environments on diversity parameters is discussed. Finally, conclusions are drawn in Section 5.
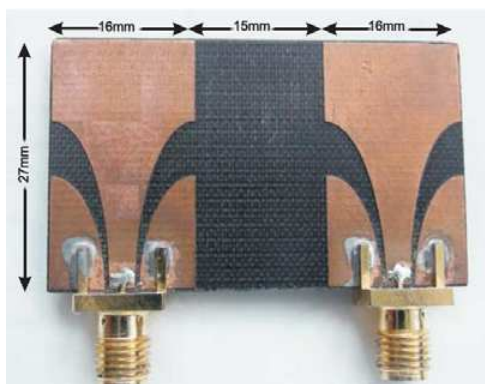


**Figure 1.** Two-branch UWB tapered slot antenna used in the experimental investigation of spatial diversity for on-body radio propagation channels.

## 2. UWB ON-BODY DIVERSITY MEASUREMENT SETTINGS

The UWB on-body diversity measurements were performed over the frequency band 3–10 GHz using tapered slot antennas (TSAs). The TSA operates in the frequency range 2.2–11 GHz with excellent impedance matching, constant gain and radiation performance across the whole band [26, 27]. The total antenna size is 27 mm × 16 mm. Unlike the traditional CPW-fed antenna, the TSA is designed to allow for the smooth transition of line impedance [26]. Figure 1 shows an example of a spatial-diversity antenna with a spacing of $0.34\lambda$ (15 mm) (where $\lambda$ is free space wavelength, the radiation pattern for the two diversity antennas were similar). Measurements were first performed in the anechoic chamber and repeated in the Body-Centric Wireless Sensor Lab at Queen Mary, University of London (Figure 3); this allowed the effects of the indoor environment on the on-body radio propagation channel to be investigated. A single tapered slot antenna (TSA) was used as the transmitter (Tx) antenna (connected to port 2 of PNA), while a two-branch diversity TSA antenna, with various spacings, was used for the receiver (Rx) antenna connected to port 1 and port 3 of PNA (as shown in Figure 2). The position of Tx was fixed at the left side of the waist. The receiving antenna was placed at five different positions: on the right chest (Rx1); right wrist (Rx2); right ankle (Rx3); on the centre of the back (Rx4); and on the right side of the head (Rx5), as shown in Figure 2.
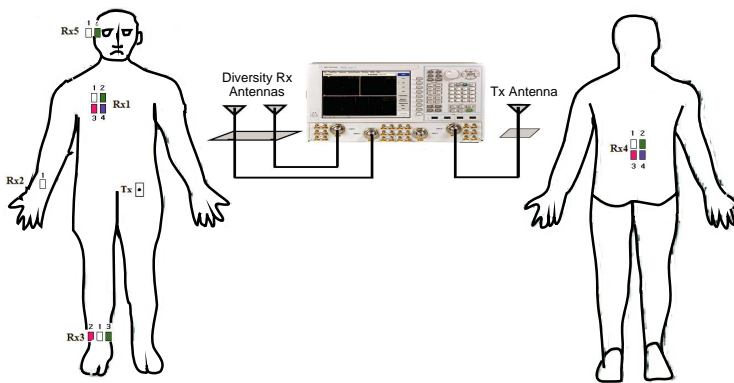


**Figure 2.** Measurement set-up used for UWB on-body diversity measurements, including position of diversity branch antennas and transmitter on the body, for both anechoic chamber and indoor environment scenarios.
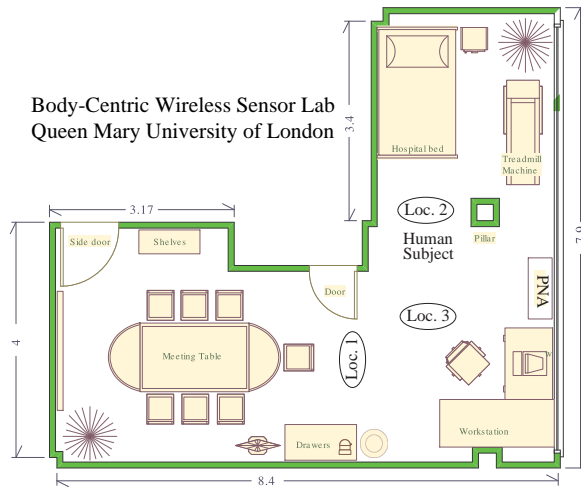
**Figure 3.** Indoor environment showing different locations of human subject for on-body diversity measurements.

A number of measurements were made for each Rx position, to check the reliability of the measurements with respect to slight variations in the position of the antenna on the body; this was achieved using a small grid, so that the variation was controlled (this was done to check the effect of accidental variation in the antenna position on diversity gain and different parameters). Measurements were repeated in three different locations in the indoor environment (denoted in Figure 3 as loc1, loc2 and loc3, respectively) to highlight the effect of varying multipath environments on the diversity measurements and results. These three locations are being selected carefully, based on the difference in the multipath components that are generated due to different surrounding environment in these three locations. In addition, the repeatability of the measurements with respect to time was investigated by repeating the measurement procedures on different days. To investigate the pseudo-dynamic nature of the UWB on-body channel with diversity techniques, a variety of movements were included, such as walking, talking on the phone, looking at a wrist-watch, running, eating and typing for a fixed period of time.

An Agilent four-port PNA-X (Programmable Vector Network Analyzer), model number N5244A, was used to capture the frequency response of the two diversity branches simultaneously, as shown in Figure 2. The PNA was remotely controlled by computer software written by author in Labview$^{TM}$ version 8.5. The data measured by the PNA was stored in the computer hard disk by the Labview$^{TM}$

software in the form of a .s4p files containing the magnitude (in dB) and phase (in degrees) of all transmission responses. During the measurements, the PNA was always calibrated to exclude the losses that incurred in the cables and thus the measured data reflects the signal measured at the ports of the antenna. The calibration also ensured that a total power of 0 dBm is transmitted by the transmitting antenna. The PNA was set to capture 3201 data samples, with a sampling time of 6.6 ms. The sampling time was carefully chosen to capture all variations made by any fast movements of the human subject and to keep the sampling frequency higher (at least double) than the resulting doppler shift. The doppler shift is discussed later, in Section 3.2. Measurements were performed in a controlled indoor environment (i.e., not in the real environment) under time varying human body channel, when surrounding environment was completely static. Measurements were taken in the Body-Centric Wireless Sensor Lab at Queen Mary, University of London, (Figure 3) in the evening time to avoid any variations in the surrounding environment due to other people movements. The goal was to investigate the potential improvement achieved by using diversity for body-centric wireless communications.

## 3. DIVERSITY TECHNIQUE ANALYSIS

### 3.1. Mutual Coupling between Diversity Branch Antennas

A spacing of $\lambda/2$ between diversity branch antenna is considered as sufficient for minimizing the effect of mutual coupling [3]. For the five on-body links (i.e., chest-to-waist, back-to-waist, wrist-to-waist, head-to-waist and ankle-to-waist), the spacing between the two branches was varied from 5 mm ($0.11\lambda$) to 32 mm ($0.73\lambda$) and the mutual coupling measured; $\lambda$ is the free-space wavelength at the centre frequency of 6.85 GHz. Result shows that, for a minimum spacing of 15 mm ($0.34\lambda$) between diversity branch antennas, the mutual coupling remained below $-15$ dB across the whole UWB band. This indicates that the antennas are suitably decoupled.

Figure 4 shows the measured mutual coupling for the five different on-body channels for location 2 (see Figure 3) at a spacing of $0.34\lambda$ between diversity branch antennas. The differences observed in the mutual coupling for the five on-body channels are mainly attributed to variation in the effective permittivity surrounding the antenna elements, due to changes in the tissue properties in the chosen on-body positions. However, for all measured on-body channels, the mutual coupling remained below $-15$ dB. Therefore, for the following
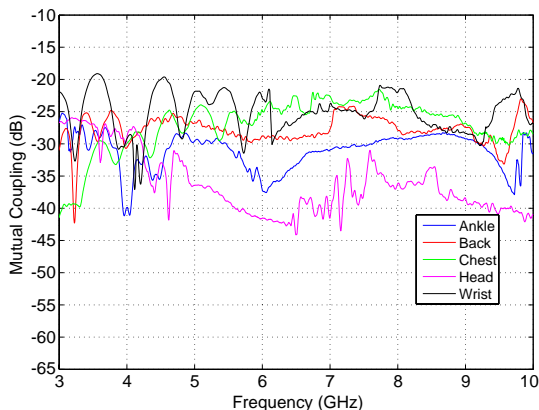
**Figure 4.** Mutual coupling for five positions of Rx with respect to Tx on the waist at location 2 in an indoor environment at $0.34\lambda$ spacing between branch antennas.

measurement campaign, a $0.34\lambda$ spacing between the branches was applied.

## 3.2. Doppler Shift

In mobile communications, a doppler shift in the signal frequency occurs due to the relative speed of motion between the transmitter and receiver; this is also true for the on-body case. In order to capture all fast movements made by the human body during measurements, the sampling frequency of the measurement should be greater than twice the maximum expected doppler shift. This shift is calculated for all channels using Eq. (1), as given in [9]:

$$f_m = \frac{v}{\lambda} \tag{1}$$

where $v$ is the velocity of motion of the human body in metres per second and $\lambda$ the wavelength in metres. For the UWB band (3.1 to 10.6 GHz), with a centre frequency of 6.85 GHz, $f_m = 22.83$ Hz for an average speed of 1 m/s and $f_m = 68.5$ Hz for a speed of 3 m/s (these speeds are calculated by using treadmill machine, based on walking speed of different subjects). The maximum Doppler shift is observed for the waist-to-wrist channel, compared to the other channels. During measurements, the sampling time was set to 6.6 ms on the PNA, to capture even the fastest movement of 3 m/s by keeping the sampling frequency equal to 150 Hz, which is greater than twice the maximum expected Doppler shift (i.e., 68.5 Hz).

### 3.3. Envelope Correlation Coefficients

Signal decorrelation is usually introduced by multipath components. To maximize the diversity gain, a low spatial correlation is needed [22]. The diversity gain for two uncorrelated branches is high, compared to correlated branches. The envelope correlation coefficient $\rho_e$ between the two diversity branches is calculated from [12]:

$$\rho_e = \frac{\sum_{i=1}^{N}(r_1(i) - \overline{r_1})(r_2(i) - \overline{r_2})}{\sqrt{\sum_{i=1}^{N}(r_1(i) - \overline{r_1})^2}\sqrt{\sum_{i=1}^{N}(r_2(i) - \overline{r_2})^2}} \tag{2}$$

where $N$ is the total number of samples and $\overline{r_j}$ the mean value of the fast-fading envelope $r_j$ for the received diversity branch signal $j$.

### 3.4. Diversity Combining and Diversity Gain Calculation

Three commonly-used diversity combining techniques are used in this paper: selection combining (SC), equal-gain combining (EGC) and maximum-ratio combining (MRC). The channel responses for the two diversity branches are captured by the PNA in the frequency domain and converted to the time domain using an Inverse Fast Fourier Transform (IFFT). Diversity combining is achieved by using the expressions given in [6] for combining the time domain signal:

$$\text{SC}(t) = \max(r_1(t), r_2(t)) \tag{3}$$

$$\text{EGC}(t) = \frac{r_1(t) + r_2(t)}{\sqrt{2}} \tag{4}$$

$$\text{MRC}(t) = \sqrt{r_1^2(t) + r_2^2(t)} \tag{5}$$

where $r_1(t)$ and $r_2(t)$ are the two received branch signal envelopes. The DG was calculated by plotting the cumulative distribution functions (CDFs) of the two branch signals and the diversity-combined signal. The DG is the difference between the strongest of the two branch signals and the diversity-combined signal at some specified outage probability [6, 7]. In this paper, the outage probability is assumed to be 10% for the DG calculation.

For MRC and EGC, co-phasing of the two branch signals was achieved by shifting the phase of one signal with respect to other signal using the simple procedure given in [3]. Figure 5 shows the CDF plot for the head-to-waist channel for the indoor environment (at Location 1). Figure 5 shows the DG calculation (which is calculated by taking the difference of strongest of two branch signals and diversity combined signal at outage probability of 10%) for head-to-waist link. DG is calculated in same manner for all other links.
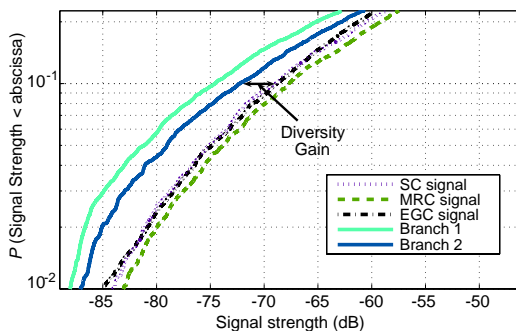
**Figure 5.** CDF plot for diversity gain calculation for head-to-waist channel, when Rx is at position 1 and the subject is at location 1.

## 4. EVALUATION OF THE DIVERSITY SCHEME AND ON-BODY RADIO CHANNEL CHARACTERISTICS

### 4.1. Impact of Branch Spacing on Diversity Parameters

Table 1 lists the DG values (for all three combining techniques), $\rho_e$ and the power imbalance between the two branches for the five on-body channels, for different spacings between diversity branch antennas, at location 2. In Table 1, power imbalance is calculated by using the ratio of the mean power of the two branch signal envelopes (i.e., absolute value of ratio $(r_1/r_2)$, where $r_1$ and $r_2$ are the mean power of two branch signal envelopes respectively).

From Table 1, it can be seen that, for almost all channels, the correlation between the diversity branch signals is lower at $0.48\lambda$ than at $0.34\lambda$, but there is an increase in the power imbalance for $0.48\lambda$ case that reduces the DG slightly (as shown in Table 1). Thus, a $0.34\lambda$ spacing is a good choice, due to the compactness of the diversity antennas and the relatively-high diversity gain. This spacing gives similar performance to the highest spacing possible; as described in Section 3.1, the mutual coupling remains below $-15$ dB for all links at this spacing.

By observing the MRC diversity gains against the antenna spacing (from results in Table 1) for the five channels tested in an indoor environment, it can be seen that the DG tends to increase slightly with increased antenna spacing. There are a few exceptions, however, in which either the power imbalance is larger or the correlation is high, hence reducing overall DG. Table 1 also shows the relationship between envelope correlation coefficient and power imbalance, respectively, with antenna spacing. It seems that the inter-spacing does not play any vital role in the spatial correlation, as predicted by [22].

**Table 1.** Diversity parameters for 5 different links at location 2 with different spacings in an indoor environment.

| Links | Results | Antenna Spacing (in terms of $\lambda$) | | | | | |
|---|---|---|---|---|---|---|---|
| | | **0.116** | **0.23** | **0.34** | **0.48** | **0.58** | **0.73** |
| **Chest-Waist** | **MRC (dB)** | 4.03 | 2.85 | 2.98 | 2.32 | 2.59 | 1.22 |
| | **EGC (dB)** | 2.91 | 2.10 | 2.45 | 3.68 | 1.71 | 0.5 |
| | **SC (dB)** | 1.92 | 2.04 | 1.38 | 3.04 | 0.83 | 0.25 |
| | $\rho_e$ | 0.625 | 0.684 | 0.686 | 0.630 | 0.668 | 0.711 |
| | **Imbalance (dB)** | 2.37 | 1.13 | 2.13 | 3.14 | 3.87 | 3.04 |
| **Head-Waist** | **MRC (dB)** | 3.45 | 3.34 | 5.02 | 4.33 | 2.17 | 2.16 |
| | **EGC (dB)** | 2.73 | 1.02 | 4.93 | 3.42 | 0.79 | 1.90 |
| | **SC (dB)** | 1.96 | 0.48 | 4.19 | 2.14 | 0.49 | 1.17 |
| | $\rho_e$ | 0.631 | 0.675 | 0.645 | 0.638 | 0.686 | 0.677 |
| | **Imbalance (dB)** | 3.99 | 2.47 | 1.11 | 1.34 | 1.92 | 2.22 |
| **Wrist-Waist** | **MRC (dB)** | 1.65 | 2.23 | 2.98 | 2.99 | 3.22 | 3.44 |
| | **EGC (dB)** | 0.68 | 1.49 | 2.09 | 1.81 | 1.40 | 2.93 |
| | **SC (dB)** | 0.57 | 0.90 | 0.92 | 1.01 | 0.98 | 2.45 |
| | $\rho_e$ | 0.691 | 0.730 | 0.697 | 0.736 | 0.734 | 0.755 |
| | **Imbalance (dB)** | 2.55 | 3.83 | 2.75 | 3.53 | 3.20 | 4.47 |
| **Ankle-Waist** | **MRC (dB)** | 3.24 | 3.70 | 4.02 | 2.56 | 3.96 | 3.03 |
| | **EGC (dB)** | 2.1 | 2.35 | 2.79 | 2.32 | 2.73 | 2.14 |
| | **SC (dB)** | 1.54 | 1.28 | 2.11 | 1.40 | 2.65 | 1.01 |
| | $\rho_e$ | 0.613 | 0.621 | 0.637 | 0.626 | 0.649 | 0.733 |
| | **Imbalance (dB)** | 3.77 | 4.84 | 4.95 | 6.56 | 6.0 | 4.63 |
| **Back-Waist** | **MRC (dB)** | 4.10 | 6.75 | 6.97 | 6.03 | 6.69 | 5.94 |
| | **EGC (dB)** | 3.56 | 6.38 | 5.76 | 5.53 | 6.21 | 4.88 |
| | **SC (dB)** | 1.33 | 4.90 | 4.11 | 3.97 | 4.15 | 3.72 |
| | $\rho_e$ | 0.604 | 0.614 | 0.618 | 0.627 | 0.630 | 0.626 |
| | **Imbalance (dB)** | 3.83 | 0.28 | 0.63 | 0.95 | 0.31 | 0.67 |

Power imbalance seems to be increasing for most of the cases because of the change of distance between Tx and Rx: one Rx antenna is closer to the Tx than the other. The variation of MRC-DG with inter-spacing is above 50% for the channels that have a LOS, or partial

LOS, link with Tx; this percentage is calculated by taking the difference between maximum and minimum DG for each link. The exception is the ankle case, where reflections from the ground make the DG process more stable.

## 4.2. Reliability of Diversity Measurements with Respect to Small On-body Position Changes

In order to ensure that all measurements are reliable, a small grid incorporating the Rx antenna was made, to see how small variations in the position of the diversity antenna affect the measurement of diversity gain. For specific cases, such as the chest and the back (see Figure 2), a $2 \times 2$ grid was applied with an approximate spacing distance of 5 mm; in the case of the ankle and the head, a one dimensional grid was used, with a similar spacing. These grids were adopted in this work to investigate the correlation coefficient between the received signals on different branches and to highlight the stability of the channel within a small window of positions in on-body measurements.

Table 2 shows that the lowest value of DG is obtained in the chest-to-waist link, when there is a LOS link between Tx and Rx. This lowest value is due to the higher power imbalance and higher

**Table 2.** Diversity parameters for different Rx positions with respect to Tx on waist in an indoor environment for location 1 at $0.34\lambda$ spacing.

| Channels | Chest | | | | Head | | Wrist | Ankle | | | Back | | | |
|---|---|---|---|---|---|---|---|---|---|---|---|---|---|---|
| | 1 | 2 | 3 | 4 | 1 | 2 | 1 | 1 | 2 | 3 | 1 | 2 | 3 | 4 |
| DG MRC (dB) | 2.52 | 2.79 | 2.74 | 3.32 | 4.62 | 4.76 | 4.35 | 4.89 | 4.38 | 4.29 | 5.27 | 4.85 | 5.22 | 4.87 |
| DG EGC (dB) | 2.06 | 2.17 | 2.28 | 3.22 | 3.48 | 3.28 | 4.02 | 4.32 | 4.12 | 4.03 | 4.48 | 4.22 | 4.43 | 4.13 |
| DG SC (dB) | 1.11 | 1.52 | 1.13 | 1.63 | 3.3 | 1.76 | 1.42 | 2.32 | 2.12 | 1.98 | 2.92 | 3.02 | 2.54 | 2.32 |
| $\rho_e$ | 0.670 | 0.667 | 0.653 | 0.642 | 0.694 | 0.678 | 0.702 | 0.701 | 0.698 | 0.701 | 0.646 | 0.670 | 0.648 | 0.671 |
| Mean Power $r_1$ (dB) | −31.74 | −33.53 | −35.17 | −33.01 | −36.12 | −34.32 | −43.61 | −36.20 | −36.21 | −36.48 | −47.91 | −48.82 | −47.16 | −48.12 |
| Mean Power $r_2$ (dB) | −35.10 | −30.16 | −32.66 | −29.06 | −32.78 | −32.83 | −41.99 | −38.22 | −39.12 | −33.74 | −48.86 | −48.34 | −49.13 | −49.92 |
| Power imbalance (dB) | 3.36 | 3.37 | 2.51 | 3.95 | 3.34 | 1.49 | 1.17 | 2.02 | 2.91 | 2.74 | 0.95 | 0.48 | 1.97 | 1.8 |

**Table 3.** Diversity parameters for different Rx positions with respect to Tx on waist in an anechoic chamber at $0.34\lambda$ spacing.

| Channels | Chest | | | | Head | | Wrist | Ankle | | | Back | | | |
|---|---|---|---|---|---|---|---|---|---|---|---|---|---|---|
| | 1 | 2 | 3 | 4 | 1 | 2 | 1 | 1 | 2 | 3 | 1 | 2 | 3 | 4 |
| DG MRC (dB) | 1.10 | 1.25 | 1.5 | 1 | 1.28 | 1.27 | 1.47 | 1.52 | 1.42 | 1.6 | 1.93 | 2.02 | 1.96 | 1.92 |
| DG EGC (dB) | 0.5 | 0.6 | 0.5 | 0.75 | 1.22 | 1.01 | 1.22 | 0.64 | 0.52 | 0.57 | 0.53 | 1.87 | 1.82 | 1.76 |
| DGSC (dB) | 0.0 | 0.1 | 0.0 | 0.0 | 0.36 | 0.34 | 0.1 | 0.0 | 0.0 | 0.0 | 0.56 | 0.54 | 0.5 | 0.5 |
| $\rho_e$ | 0.640 | 0.640 | 0.641 | 0.640 | 0.720 | 0.721 | 0.730 | 0.746 | 0.746 | 0.745 | 0.650 | 0.650 | 0.651 | 0.648 |
| Mean Power $r_1$ (dB) | −29.15 | −29.16 | −29.24 | −29.16 | −39.58 | −39.85 | −44.77 | −39.74 | −39.76 | −39.84 | −47.34 | −47.46 | −47.12 | −47.38 |
| Mean Power $r_2$ (dB) | −34.66 | −34.68 | −34.52 | −33.99 | −37.85 | −37.55 | −42.53 | −39.65 | −39.72 | −39.52 | −48.14 | −48.24 | −47.98 | −47.02 |
| Power imbalance (dB) | 5.51 | 5.52 | 5.28 | 4.83 | 1.73 | 2.3 | 2.24 | 0.09 | 0.04 | 0.32 | 0.8 | 0.78 | 0.86 | 0.36 |

correlation, which result from dominant direct rays, compared to multipath components. The highest value of DG is obtained in the back-to-waist channel, which is a NLOS channel. The higher value of DG and low power imbalance suggest that signals are reasonably uncorrelated and also movements of body parts result in higher decorrelation between the two branch signals. For all other partial LOS channels (i.e., the wrist-, ankle- and head-to-waist cases), the DG lies between the chest-to-waist and back-to-waist channels. This is due to fact that multipath components are slightly dominating in these cases, because of scattering from different parts of human body and the rich scattering environment.

Table 3 shows the diversity gain using different combining techniques and diversity parameters in an anechoic chamber, at $0.34\lambda$ spacing between diversity branch antennas. Very low values of diversity gain for all cases, compared to those found in the indoor environment, confirm the expectation that there are no reflections from the surrounding environment and that the only source of multipath components in the anechoic chamber was the human body itself. The differences in DG observed between the different on-body channels are due to the same causes described for the indoor environment in the above paragraph.

Tables 2 and 3 show that, due to the variation in Rx antenna position on the body, the MRC-DG changes from 0.01 dB to 0.5 dB for the anechoic chamber case and 0.14 dB to 0.8 dB for the indoor environment. Results therefore show that variation of Rx antenna position will not severely affect the measurement of DG. For the remaining results, we consider only position 2 (Figure 2) for each Rx location.

## 4.3. Comparison of Diversity Gain for the Free Space and Indoor Environments

A comparison of MRC-DG is shown in Figure 6 for five different Rx positions (position 2 for each Rx is taken as shown in Figure 2), in both the anechoic chamber and three different locations in an indoor environment, with respect to Tx on the waist. Low values of DG in the chamber are due to less scattering from the surrounding environment, compared to the indoor case, where there are rich multipath reflections. In the chamber, only reflections from human body parts due to movement play a role in acquiring DG; in an indoor environment, both the human body parts and surrounding environment contribute to DG. This shows the fact that diversity is useful only when the human subject is present in rich multipath environments. Also, moderate values of DG in the anechoic chamber confirms both the presence of
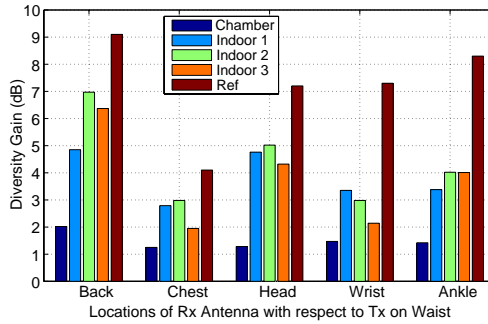
**Figure 6.** Comparison of MRC diversity gain for different links for position 2 and three locations at $0.34\lambda$ spacing in an indoor environment in comparison with Ref, which is DG at $2.45\,$GHz in an indoor environment presented in [2].

**Table 4.** Diversity parameters for three different locations at $0.34\lambda$ spacing between diversity branch Rx in an indoor environment.

| | Chest-Waist | | | Head-Waist | | | Wrist-Waist | | | Ankle-Waist | | | Back-Waist | | |
|---|---|---|---|---|---|---|---|---|---|---|---|---|---|---|---|
| Locations | 1 | 2 | 3 | 1 | 2 | 3 | 1 | 2 | 3 | 1 | 2 | 3 | 1 | 2 | 3 |
| MRC (dB) | 2.79 | 2.98 | 1.95 | 4.76 | 5.02 | 4.32 | 3.35 | 2.98 | 2.14 | 3.38 | 4.02 | 4.01 | 4.85 | 6.97 | 6.37 |
| EGC (dB) | 2.17 | 2.45 | 1.15 | 3.28 | 4.43 | 3.14 | 3.02 | 2.09 | 2.01 | 3.12 | 2.79 | 2.77 | 4.22 | 5.76 | 5.44 |
| SC (dB) | 1.11 | 1.38 | 0.98 | 1.76 | 4.19 | 3.04 | 1.42 | 0.92 | 1.19 | 2.12 | 2.11 | 2.50 | 3.02 | 4.11 | 3.87 |
| $\rho_e$ | 0.670 | 0.686 | 0.661 | 0.678 | 0.645 | 0.637 | 0.702 | 0.697 | 0.678 | 0.698 | 0.637 | 0.636 | 0.670 | 0.618 | 0.685 |
| $r_1$ (dB) | −31.74 | −31 | −28.71 | −34.32 | −27.55 | −36.41 | −43.61 | −32 | −38.35 | −36.21 | −35.23 | −31.98 | −48.82 | −47.23 | −47.67 |
| $r_2$ (dB) | −35.10 | −33.14 | −26.21 | −32.83 | −26.43 | −32.58 | −41.99 | −35.08 | −40.67 | −39.12 | −30.20 | −28.96 | −48.34 | −46.60 | −48.35 |
| Imbalance(dB) | 3.36 | 2.13 | 2.50 | 3.34 | 1.11 | 3.83 | 1.17 | 3.08 | 3.02 | 2.91 | 4.95 | 3.02 | 0.48 | 0.63 | 0.78 |

multipath components due to the movement of body parts and the fact that their contribution to DG is not the dominant factor in more realistic environments.

## 4.4. Effect of Different Subject Locations on UWB Diversity Gain

Table 4 shows the diversity parameters for $0.34\lambda$ spacing between diversity branch antennas at three different locations in an indoor environment (Figure 3). The highest DG values are obtained for location 2, because the subject is close to the walls and the pillar in this case, leading to stronger multipath reflections. The wrist-to-waist channel is the exception: here, DG is low, compared to other locations, due to the higher power imbalance and higher correlation in this case, as the wrist was very close to the wall.

The highest value of DG (i.e., $6.97\,$dB using MRC) is obtained for

the back-to-waist link (NLOS case), compared to the other links for location 2. The higher value of DG and low power imbalance (0.63 dB) for back-to-waist link suggests that signals are reasonably uncorrelated and also that movements of body parts result in a higher decorrelation between the two branch signals. The same reasoning as described in Section 4.2 can be applied to account for DG variation for all other links.

The results obtained for UWB on-body diversity at location 2 are compared with the results of Khan et al. at 2.4 GHz presented in [2] in an indoor environment (comparison plot is shown in Figure 6). This is an approximate comparison; as for both measurement results, human subject and indoor environment were different). Results approximately agree for the chest-to-waist link (where there is direct LOS communication between Tx and Rx). However, there is disagreement for partial LOS cases and NLOS case (i.e., the head-to-waist, wrist-to-waist and back-to-waist links); this is due to the fact that, for NLOS cases, the reflections and contributions by the environment have a large effect on the quality of the signal and the measurements were done in different environments. In addition, the subject-specific behaviour of the UWB on-body channel (see, for example, the work of Sani et al. [28]) will also play role in explaining the disagreement between the results.

## 5. CONCLUSION

Spatial diversity techniques for ultra-wideband on-body radio channels have been investigated and analysed in this paper. Various scenarios, including changes in antenna on-body positions, the location of subject in the indoor environment and also variation in the inter-spacing between antenna element branches, have been considered. Results showed that, for dense multipath environments, the benefits of applying diversity techniques were significant for the non-line-of-sight cases, where there are low power imbalances due to uncorrelated signals, in comparison to the line-of-sight scenarios. Maximum variations of 0.5 dB and 0.8 dB, for the anechoic chamber and the indoor environment cases, respectively, have been observed in response to slight changes in the on-body antenna position. This demonstrated the potentially negligible effect of accidental and inherited on-body element location shift due to the subject's sudden movement. The results presented in this paper gave indications of the beneficial applications of diversity antenna techniques for potential performance enhancement of UWB body-centric wireless communications as experienced in narrowband technologies. This will be increasingly

appreciated for off-body communications, due to the variation in the spatial and angular parameters of the multipath components that will contribute to enhanced diversity gain.

# REFERENCES

1. Hall, P. S. and Y. Hao, *Antennas and Propagation for Body-centric Wireless Communications*, Artech House, 2006.

2. Khan, I., P. S. Hall, A. A. Serra, A. R. Guraliuc, and P. Nepa, "Diversity performance analysis for on-body communication channels at 2.45 GHz," *IEEE Transactions on Antennas and Propagation*, Vol. 57, No. 4, 956–963, Apr. 2009.

3. Jakes, W. C., *Microwave Mobile Communications*, Wiley, New York, 1974.

4. Allen, B., M. Dohler, E. Okon, W. Q. Malik, A. K. Brown, and D. Edwards, *UWB Antenna and Propagation for Communications, Radar and Imaging,* John Wiley & Sons Ltd., 2007.

5. Vaughan, R. G. and J. B. Andersen, "Antenna diversity in mobile communications," *IEEE Transactions on Vehicular Technology*, Vol. 36, No. 4, 149–172, Nov. 1987.

6. Khan, I. and P. S. Hall, "Multiple antenna reception at 5.8 and 10 GHz for body-centric wireless communication channels," *IEEE Transactions on Antennas and Propagation*, Vol. 57, No. 1, 248–255, Jan. 2009.

7. Correia, L. M., *Mobile Broadband Multimedia Networks Techniques, Models and Tools for 4G*, Elsevier Ltd., 2006.

8. Colburn, J. S., Y. Rahmat-Samii, M. A. Jensen, and G. J. Pottie, "Evaluation of personal communications dual-antenna handset diversity performance," *IEEE Transactions on Vehicular Technology*, Vol. 47, No. 3, 737–746, Aug. 1998.

9. Rappaport, T. S., *Wireless Communications Principles and Practice*, Prentice Hall, Inc., New Jersey, 1996.

10. Dietrich, C. B. J., K. Dietze, J. R. Nealy, and W. L. Stutzman, "Spatial, polarization, and pattern diversity for wireless handheld terminals," *IEEE Transactions on Antennas and Propagation*, Vol. 49, No. 9, 1271–1281, Sep. 2001.

11. Karaboikis, M., C. Soras, G. Tsachtsiris, and V. Makios, "Three-branch antenna diversity systems on wireless devices using various printed monopoles," *IEEE International Symposium on Electromagnetic Compatibility*, May 11–16, 2003.

12. Turkmani, A. M. D., A. A. Arowojolu, P. A. Jefford, and

C. J. Kellett, "An experimental evaluation of the performance of two-branch space and polarization diversity schemes at 1800 MHz," *IEEE Transactions on Vehicular Technology*, Vol. 44, No. 2, 318–326, May 1995.

13. Serra, A. A., P. Nepa, G. Manara, and P. Hall, "Diversity measurements for on-body communication systems," *IEEE Antennas and Wireless Propagation Letters*, Vol. 6, No. 1, 361–363, Jan. 2007.

14. Cotton, S. L. and W. G. Scanlon, "Channel characterization for singleand multiple-antenna wearable systems used for indoor body-to-body communications," *IEEE Transactions on Antennas and Propagation*, Vol. 57, No. 4, 980–990, Jan. 2009.

15. Cotton, L. and G. Scanlon, "Characterization and modeling of onbody spatial diversity within indoor environments at 868 MHz," *IEEE Transactions on Wireless Communications*, Vol. 8, No. 1, 176–185, Jan. 2009.

16. Kaiser, T. and F. Zheng, *Ultra Wideband Systems with MIMO*, John Wiley & Sons Ltd., 2010.

17. Chang, W. J., J. H. Tarng, and S. Y. Peng, "Frequency-space-polarization on UWB mimo performance for body area network applications," *IEEE Antennas and Wireless Propagation Letters*, Vol. 7, 577–580, Jan. 2009.

18. Sibille, A. and S. Bories, "Spatial diversity for UWB communications," *5th European (Conf. Publ. No. 492) Personal Mobile Communications Conference*, 367–370, 2003.

19. D'Errico, R., A. Sibille, A. Giorgetti, and M. Chiani, "Antenna diversity in UWB indoor channel," *IEEE International Conference on Ultra-wideband, ICUWB*, 13–16, 2008.

20. Chen, Y., J. Teo, J. C. Y. Lai, E. Gunawan, S. L. Kay, B. S. Cheong, and P. B. Rapajic, "Cooperative communications in ultra-wideband wireless body area networks: Channel modeling and system diversity analysis," *IEEE Journal on Selected Areas in Communications*, Vol. 27, No. 1, 5–16, Jan. 2009.

21. Maria-Gabriella, D. B., T. Kaiser, A. F. Molish, I. Oppermann, C. Politan, and D. Porcino, *UWB Communication Systems: A Comprehensive Overview*, Hindawi Publishing Corporation, 2006.

22. Roy, V., S. Oestges, C. Horlin, F. Doncker, and P. Opera, "Ultrawideband spatial channel characterization for body area networks," *Proceedings of European Conference on Antennas and Propagation (EuCAP)*, Edinburgh, UK, Nov. 11–16, 2007.

23. Van Roy, S., C. Oestges, F. Horlin, and P. de Doncker, "A

comprehensive channel model for UWB multisensor multiantenna body area networks," *IEEE Transactions on Antennas and Propagation*, Vol. 58, No. 1, 163–170, Jan. 2010.

24. Abbasi, Q. H., A. Alomainy, and Y. Hao, "Antenna diversity technique for enhanced ultra wideband radio performance in body-centric wireless networks," *European Wireless Technology Conference (EuWIT)*, Paris, France, Nov. 27–28, 2010.

25. Abbasi, Q. H., A. Alomainy, and Y. Hao, "Ultra wideband antenna diversity techniques for on/off-body radio channel characterisation," *IEEE International Workshop on Antenna Technology (iWAT)*, 209–212, Hong Kong, Mar. 5–7, 2012.

26. Rahman, A., A. Alomainy, and Y. Hao, "Compact body-worn coplanar waveguide fed antenna for UWB body-centric wireless communications," *Proceedings of European Conference on Antennas and Propagation (EuCAP)*, Edinburgh, U.K., Nov. 11–16, 2007.

27. Alomainy, A., A. Sani, J. Santas, A. Rahman, and Y. Hao, "Transient characteristics of wearable antennas and radio propagation channels for ultra wideband body-centric wireless communications," *IEEE Transactions on Antennas and Propagation*, Vol. 57, No. 1, 875–884, Apr. 2009.

28. Sani, A., Y. Hao, Y. Zhao, S. L. Lee, and G. Z. Yang, "A subject-specific numerical study in UWB body-centric wireless communications," *Proceedings of the Fourth European Conference on Antennas and Propagation (EuCAP)*, Barcelona, Spain, Apr. 12–16, 2010.